International Journal Of
Industrial Electronics Control and Optimization
Print ISSN: 3517-2645
Online ISSN: 3568-2645
Homepage: https://ieco.usb.ac.ir/

Controlling the Ground Particle Size and Ball Mill Load Based on Acoustic Signal, Quantum Computation Basis, and Least Squares Regression, Case Study: Lakan Lead-Zinc Processing Plant

Sadegh Kalantari[1] | Ali Madadi[2] | Mehdi Ramezani[3] | Abdolmotaleb Hajati[4]
Department of Electrical Engineering, Tafresh University, Tafresh, Iran.[1, 2]
Department of Mathematics, Tafresh University, Tafresh, Iran.[3]
Department of Mining Engineering, Arak University of Technology, Arak, Iran.[4]
Corresponding author's email: Ramezani@tafreshu.ac.ir

Article Info

Article type:
Research Article

Article history:
Received: 24-June-2023
Received in revised form: 13-September-2023
Accepted: 15-Sep-2023
Published online: 19-Sep-2023

Keywords:
Least Squares Regression, Quantum Computation,Ball Mill System Identification, Acoustic Signal, Ball Mill Control

ABSTRACT

Grinding in a ball mill is a process with high energy consumption; therefore, a slight improvement in its performance can lead to significant economic benefits in the industry. The softness of the product of the grinding circuits prevents loss of energy in the subsequent processes. In addition, controlling the mill's performance is challenging due to its complex dynamic characteristics. The primary purpose of this article is to use the ground particle size diagram and acoustic signal in ball mill control, and model their relationship based on the least squares method. As a result, by extracting valuable data from the acoustic signal, the optimal condition of the ball mill_ in terms of ground particle size and ball mill load (standard, low, high)_ can be achieved. In doing so, in this article, innovative ideas such as adaptive quantum basis, sparse representation, SVD, and PCA-based methods were used. The proposed method has been practically implemented on the ball mill of the Lakan lead-zinc processing plant. Also, a prototype of the device was built. The test results show that the optimal load for the studied ball mill is 10t/h. In this case, the ground particle size is 110-120 microns, which is ideal for this plant. Also, the power spectrum is in the middle-frequency band (300-700 Hz). According to the analysis and results, the proposed method will increase the efficiency of the studied ball mill.

I. Introduction

A. Background

In mineral processing, particles containing valuable minerals must be ground to reach a size that is small enough to be released from the tailings and easily separated by a suitable concentration method [1, 2]. Grinding is a critical operation in mineral processing, which has a considerable impact on the economic value of the product. Many industrial surveys have proven that the grinding process accounts for a significant part of the total cost of metal production [3, 4]. Impact and friction are the primary mechanisms for size reduction in grinding. Ball milling is an essential process with more than 50% of the total energy consumption; therefore, a slight improvement in ball mill efficiency would result in a substantial economic benefit for the industry. The other important issue in the grinding process is the softness of the grinding circuit product. It affects the performance of the subsequent separation processes. Therefore, the precise control of the grinding circuits is significant to prevent energy loss and improve the efficiency of the operations. Controlling the performance of a closed

circuit ball mill is a challenging issue due to its complex dynamic characteristics and numerous interactions during the control loops [5]. Also, the variables of the ball mill cannot be easily measured due to the harsh working conditions and the impossibility of stopping it. Therefore, it is impossible to access all the variables for more accurate observation and better control of the ball mill performance. The main goal of researchers is to reduce the energy consumption of the grinding circuits, and, at the same time, to reduce the abrasion of grinding media to maintain the high quality of the final product [6, 7]. To reach this goal, a model is needed for optimal control of the ball mill regarding ground particle size and load [8]. One of the variables that has been studied by the researchers is the acoustic signal resulting from the collision of the material with the shell. The acoustic signal is a superposition of the grinding parameters, which shows the general state of the ball mill [5]. Therefore, it can indirectly express the critical condition of the ball mill operation. Although the relationship between the acoustic signal and the grinding conditions is complex, some of the ball mill characteristics can be extracted by examining the behavior of the time domain and frequency of the signal. Finally, using the acoustic signal data, the conditions inside the ball mill can be identified. Also, a suitable model can be introduced to control the ball mill system.

B. Literature Review

The acoustic signal has been studied in various researches. Recently, the relationship between sound intensity and ground particle size has been investigated in the Alumina ball mill [5]. In this paper, the critical rotation speed of the ball mill has been determined to reach the proper particle size using the sound spectrum analysis. According to this article, when the rotational speed is lower or higher than the critical speed, the size of the output particles increases, and the efficiency of the ball mill decreases accordingly. In addition, the sound intensity in critical speed is higher than the other modes. Therefore, there is a direct correlation between sound intensity and grinding efficiency [5]. Tang et al. have introduced some developments in the grinding process based on soft measuring methods such as acoustic signals and mechanical vibration [9]. In that article, techniques such as Fourier and Wavelet are reviewed to extract information from sound and vibration signals. Some offline and online models have also been presented for industrial applications. Shi et al. represented some acoustic signal measurement methods using fractional Fourier transform to detect the ball mill load [10]. The data related to load parameters are extracted by representing the signal as a fractional Fourier transform and spectrum subtractions. Characteristics of the grinding signal are obtained from the geometric spectral subtraction based on an autoregressive model in reference [11]. Using ensemble empirical mode decomposition and multi-scale spectral information, the conditions of the mill load are determined. Method [12] uses acoustic emission signals to train the convolutional neural network that can predict particle size distributions. In this method, the required data are obtained from the discrete element method and used for network training and testing.

C. Research Challenges and Motivations

Although in most of the previous research, soft measuring methods have been performed only on a laboratory sample to know the parameters of the ball mill. Here, the aim is to use such techniques in industrial applications [9]. In this paper, a new approach was implemented to control the ground particle size and feed rate (load of a ball mill) in the Lakan lead-zinc processing plant. Lakan lead-zinc processing plant is 46 kilometers southwest of Arak, a city in the central province of Iran. This factory is one of the most important sources of lead and zinc concentrate production, which started working in 1968. One of the challenges of this factory is its outdated equipment. Since the power consumption of this device is high, controlling its feed rate and output ground particle size can result in higher efficiency and lower energy consumption. Therefore, this article aims to present an effective method for optimal control of ball mills. To control the ball milling operation, parameters such as input feed rate, input water, rotational speed, and ball mill particle size distribution are the minimum requirements [8]. The specifications of the studied ball mill, whose liner is made of plastic, are shown in Table 1. It should be noted that the sizes of the balls are not fixed, ranging from 20 to 90 mm. The reason is that if a fixed size is used, some holes will be created between the balls, increasing the grinding time and the size of the ground particles. As illustrated, the rotational speed and input water of the ball mill studied in this article are constant; however, the feed rate can vary. Therefore, in this study, by changing the feed rate of the ball mill, we achieved optimal efficiency, and the feed rate was proved to be a critical parameter for optimal control of the ball mill.

D. Methodology

In this study, the wet ball mill efficiency of the Lakan lead-zinc processing plant is investigated according to the feed rate and the ground product, before and after the ball charging. To identify the ball mill system, it is necessary to sample the acoustic signal.

TABLE 1
CHARACTERISTICS OF THE BALL MILL

Length	2500 mm
Outer diameter	2300 mm
Gearbox input speed	1775 rpm
Output speed	21 rpm
Ball size range	20-90 mm
Thickness of body and liners	1500 mm
Liner material	Plastic

Therefore, the acoustic signal is first recorded at different times (based on retention time and under different feed rates) while the mill operates before and after the ball charge. In the meantime, the output product of the ball mill is sampled, and after sieve analysis, the distribution of ground particle size is obtained. Then, the outliers of the recorded acoustic signal are removed using a method based on quantum computation and sparse representation. In the next step, the relationship between the audio signal and ground particle size distribution is obtained using least square regression, processing the sound signal and extracting its helpful features, such as the maximum frequency component. By applying this model, the load and ground particle size ball mill can be effectively controlled. In this study, after identifying the ball mill system using an acoustic signal, an electronic control device was also built and tested. According to the test results, the presented method improved the wet ball mill efficiency of the Lakan lead-zinc processing plant. The sections of the article are organized as follows. In section 2, the proposed method is entirely explained. In section 3, the results and practical tests are presented, and conclusions are given in section 4.

II. Proposed Method

In this part, all the steps of the proposed method will be explained in detail. The proposed plan includes modeling and a ball mill control scheme. The modeling steps and ball mill control flowcharts are shown in Fig. 1 and Fig. 2, respectively. First, the system modeling is done using the steps in Fig. 1. Then, using the steps in Fig. 2, the ball mill is controlled. The central parts of the proposed method include removing outliers with the adaptive quantum basis, extracting features from the audio signal using the Fourier transform, using the PCA method to select the central part, and modeling based on the least squares.

According to Fig. 1, the first step is acoustic signal acquisition. In the next step, removing outliers and noise is performed on the signal to reduce the modeling error. The proposed method to remove noise is as follows: first, a basis (dictionary) is created using the input signal. To separate the primary information and noise, the desired signal is projected onto the dictionary. After obtaining the coefficients in the dictionary domain, the denoised signal is reconstructed. In the next step, the Fourier transform of the denoised signal is calculated. Then, several essential features are extracted from the Fourier transform. To reduce the dimensions of the features, the PCA-based method is used in the next step. Finally, using the least squares method, the relationship between particle size distribution and acoustic signal is obtained as a system model. In Fig. 2, the ball mill system is controlled using the model obtained at this step. In the following sections, the different steps will be explained.

A. Denoising Scheme

Since ball mills are applied in industrial environments, the received acoustic signals contain noise and outlier points. One of the most critical parts of the ball mill control is the noise removal step. If the acoustic signal is not correctly denoised, it can cause errors in the control system. There are different methods to remove outliers and noise in the signal. Signal decomposition is one of the most common methods of noise removal. For this purpose, methods based on Fourier, Wavelet, and SVD are usually used [13-15]. These methods use a fixed basis to represent the signal and noise removal. In this paper, we used the denoising method, which is based on an adaptive basis. Recently, quantum computing has been used in various fields. Reconstructing geological images and removing noise is one of its most important applications [16-18]. In this article, the signal is denoised by changing in the idea proposed in [18].

In the proposed method, the discrete version of the Schrodinger equation in quantum computation is used to build an adaptive basis or dictionary. Therefore, this method has the advantage of calculating the transformation compatible with the desired acoustic signal. Another reason for using this method is that it can eliminate most common noises in industrial environments, because of its adjustable parameters [18]. It should be noted that in this study, we have used the idea of [18], only to create a dictionary**.** The rest of the algorithm, which concerns noise elimination, is the innovation of this article.

B. Construction of Quantum Adaptive Basis (Dictionary)

The stationary Schrodinger equation in quantum mechanics (a quantum particle with energy E and in potential $V(r)$) is as follows:

$$-\frac{\hbar^2}{2m}\nabla^2\varphi = -V(r) + E\varphi \quad (1)$$

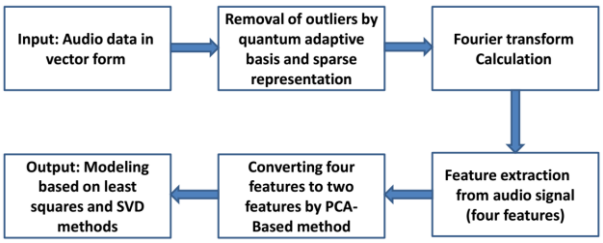

Fig. 1. Modeling flowchart of the proposed method

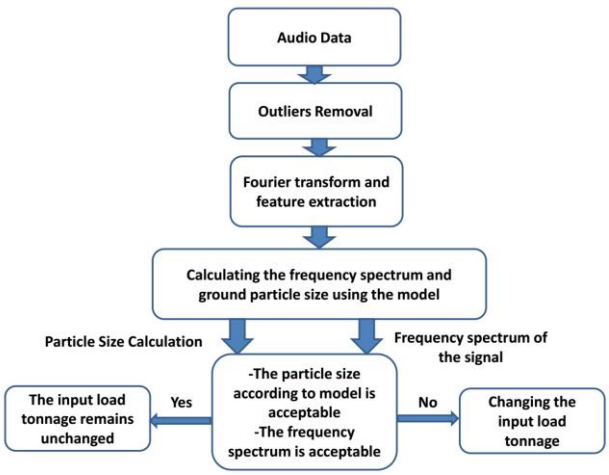

Fig. 2. Control flowchart of the proposed method

where m is the quantum particle mass, $\hbar/2\pi$ is the reduced Planck's constant, and ∇^2 is the Laplacian operator. This equation determines the wave function $\varphi(r)$ regarding spatial coordinates. To use this equation (in making the dictionary and signal denoising), the desired signal is considered a potential $V(r)$. Assuming a constant potential and a wave function with a periodicity of L, the answer to the Schrodinger equation will be in the following form:

$$\varphi(r) = Aexp(i\frac{\sqrt{2m(E-V)}}{\hbar}r) \tag{2}$$

where A is the amplitude. According to (2), by discretizing the space with N values, we will get N answers, and the frequency of the wave function will depend on $\sqrt{E-V}$. To use this equation to construct an adaptive basis, the desired signal is replaced by the potential $V(r)$. Therefore, it is necessary to create the discrete version of the Schrodinger equation. In operator form, (1) will be as follows:

$$H\varphi = E\varphi. \tag{3}$$

where $H = -\frac{\hbar^2}{2m}\nabla^2 + V$ is called the Hamiltonian operator. By replacing $y(t)$ (acoustic signal) with the size of N instead of $V(r)$, the size of H will be $N \times N$. When the discrete definitions of derivative and Laplacian are inserted, (3) will be as follows:

$$(\nabla\varphi)_t = \varphi(t+1) - \varphi(t)$$
$$(\nabla^2\varphi)_t = \varphi(t+1) - 2\varphi(t) + \varphi(t-1)$$

$$\text{Thus } (H\varphi)_t = -\frac{\hbar^2}{2m}(\varphi(t+1) - 2\varphi(t) + \varphi(t-1) + y(t)\varphi(t)) \Downarrow (H\varphi)_t = \left(y(t) + 2\frac{\hbar^2}{2m}\right)\varphi(t) - \frac{\hbar^2}{2m}\varphi(t+1) - \frac{\hbar^2}{2m}\varphi(t-1). \tag{4}$$

The simpler form of (4) is as follows:

$$(H\varphi)_t = \sum_{s=t-1}^{t+1} H(t,s)\varphi(s) \text{ for } t = 1,2,3,\dots,N. \Downarrow H(t,s) = \begin{cases} y(t) + 2\frac{\hbar^2}{2m} & for\ t = s \\ -\frac{\hbar^2}{2m} & for\ s = t+1\ and\ t = s-1 \\ 0 & otherwise \end{cases} \tag{5}$$

Therefore, the Hamiltonian matrix will be in the following form:

$$H = \begin{bmatrix} y(1) + 2\frac{\hbar^2}{2m} & -\frac{\hbar^2}{2m} & 0 \\ -\frac{\hbar^2}{2m} & \ddots & -\frac{\hbar^2}{2m} \\ 0 & -\frac{\hbar^2}{2m} & y(N) + 2\frac{\hbar^2}{2m} \end{bmatrix}. \tag{6}$$

According to (3), eigenvectors of the Hamiltonian matrix can be computed for different values of E, and they form a basis in the Hilbert space. This matrix has N eigenvectors, which are represented by φ_i. These eigenvectors form a basis, which is called a dictionary in this article. It should be noted that one of the problems of the Schrodinger equation is the localization of the basis, which is caused by the Anderson localization phenomenon [19]. To solve this problem, the input signal is first smoothed using a Gaussian filter [18]. Then, the dictionary is made from the smoothed signal. The desired audio signal will have a sparse representation in this dictionary. Using this method, the noisy and non-noisy parts are separated, and the signal will be denoised. In the following, the idea of sparse representation will be expressed.

C. Sparse Representation Model

Recently, the sparse model has been used in various applications such as reconstruction and noise removal [20-21]. In this model, $\boldsymbol{\varphi} = [\varphi_1, \dots, \varphi_N]$ represents the dictionary, φ_i is the dictionary atom with the unit norm, and $\boldsymbol{y}$ represents the vectorized signal. In sparse representation, it is assumed that the desired signal can be represented by a small number of dictionary atoms. The $\boldsymbol{y}$ signal can be represented as follows:

$$\boldsymbol{y} = \boldsymbol{\varphi}\beta = \sum_{i=1}^{N} \varphi_i \beta_i \tag{7}$$

where β will be the sparse representation of $\boldsymbol{y}$ in $\boldsymbol{\varphi}$, if it contains a few non-zero coefficients. The problem of finding β is formulated as follows:

$$\beta = argmin_{\beta} \quad \|\boldsymbol{y} - \boldsymbol{\varphi}\beta\|_2^2 \quad \text{subject to} \quad \|\beta\|_0 \leq s \qquad (8)$$

where $\|\beta\|_0$ means the number of non-zero elements of β and s is sparsity. Matching Pursuit (MP) method is commonly used to solve the above problem [20]. This method starts with finding the atom that best matches the signal. The error in this step is defined as follows:

$$E_i = min_{\alpha}\|\alpha\varphi_i - \boldsymbol{y}\| \qquad (9)$$

where α is a scalar. The above problem is solved using $\alpha^* = \langle \boldsymbol{y}, \varphi_i \rangle$, and the index of the best match is calculated as i_0. Then, the residual signal $\boldsymbol{r}$ is calculated, and this process continues until the desired accuracy is reached. The MP algorithm to achieve a sparse representation of a signal is shown in Table 2.

After calculating the sparse representation of the signal in the dictionary space, the denoised signal is obtained using $\hat{\boldsymbol{y}} = \boldsymbol{\varphi}\beta$. The steps of the proposed denoising algorithm are shown in Table 3. According to (6), the size of the Hamiltonian matrix is $N \times N$. If the size of the input signal is large, the computational complexity in dictionary construction will be very high. Therefore, in these cases, the input signal is divided into different patches, and the algorithm of Table 3 is executed on each patch. In addition to reducing the computational complexity, this method will also solve the problem of lack of memory. It should be noted that in this article, the parameters are set as $\frac{\hbar^2}{2m} = 0.4$, $\eta = 0.2$, and $\sigma = 5$.

D. Fast Fourier Transform and Feature Extraction

Fast Fourier transform is a method that computes the DFT (Discrete Fourier Transform) of a sequence [22]. It reduces the computations needed for N points from $2N^2$ to $2Nlog_2N$. Fourier analysis converts a signal from its original (often time) to the frequency domain. In this part, the fast Fourier transform of the denoised audio signal and the power spectrum are calculated. In Fig. 3, one sample of acoustic signal at different sampling times is shown along with their frequency spectrum. According to Fig. 3, at each sampling time, one component of the power spectrum is considerably different energy than the others. Therefore, the amplitude and frequency of this component are selected as the feature extracted from this sample. Two essential features of the time domain, i.e., maximum and minimum sound intensity, are also used as extracted features. Therefore, four features extracted from the acoustic signal are considered candidates. In the next step, by reducing the dimensions of the features, they are converted into two main features.

TABLE 2
MATCHING PURSUIT ALGORITHM

1. $\boldsymbol{r} = \boldsymbol{y}, \beta^1 = 0,\ z = 1$
2. ***while*** $(\boldsymbol{r} > \eta)$ ***do***
3. $E_i = min_{\alpha}\|\alpha\varphi_i - \boldsymbol{y}\|$
4. $i_0 = argmin_{\ i}E_i$
5. $\beta_i^z = \begin{cases} \beta_i^{z-1}: & i \neq i_0 \\ \beta_i^{z-1} + \langle \boldsymbol{r}, \varphi_i \rangle: & i = i_0 \end{cases}$
6. $\boldsymbol{r} = \boldsymbol{y} - \boldsymbol{\varphi}\beta^z$
7. $z = z + 1$
8. ***end while***
9. $\beta = \beta^{z-1}$

TABLE 3
PROPOSED DENOISING ALGORITHM

Input: $\boldsymbol{y}$ *(Noisy Signal),* $\frac{\hbar^2}{2m}$, η, σ

1- *Smooth the input acoustic signal with a Gaussian filter*
2- *Compute the Hamiltonian matrix using (6)*
3- *Calculate the eigenvectors of the* H *matrix (get* φ_i*)*
4- *Consider the* φ_i *vectors as a dictionary of atoms and normalize them (get* $\boldsymbol{\varphi}$*)*
5- *Get sparse representation* β *using the MP algorithm (Table 2)*
6- *Reconstruct the denoised signal using* $\hat{\boldsymbol{y}} = \boldsymbol{\varphi}\beta$

Output: $\hat{\boldsymbol{y}}$ *(Denoised Signal)*

E. Dimension Reduction Method

One essential tool to reduce the data dimensions is representation in principal component space [23]. Since the goal of this article is to model the ground particle size versus sound characteristics, data dimensions should be reduced after extracting the features. During the operation of the ball mill, the output product is sampled at different time intervals, and the audio signal is also recorded simultaneously. After sieve analysis, a particle size is assigned to each sampling time. Considering that the values of the variables were extracted from the sound at different sampling times, the data matrix size will be $M \times N$, where M is the number of observations, and N is the number of extracted features. To reduce the dimensions of the extracted features according to Table 4, the covariance matrix of the data is first calculated. Then, the eigenvectors of the covariance matrix are extracted. This matrix is called V. Finally, new data is formed by the product of X and V. In the next step, these data are used for modeling. Using this method, the principal components of the data are computed, and the dimension of the features is reduced.

F. Modeling Based on Least Squares Regression

In this part, the method of least squares in identifying the ball mill system is briefly reviewed. This method, while being simple, is good enough to control the ground particle size and ball mill load based on practical tests.

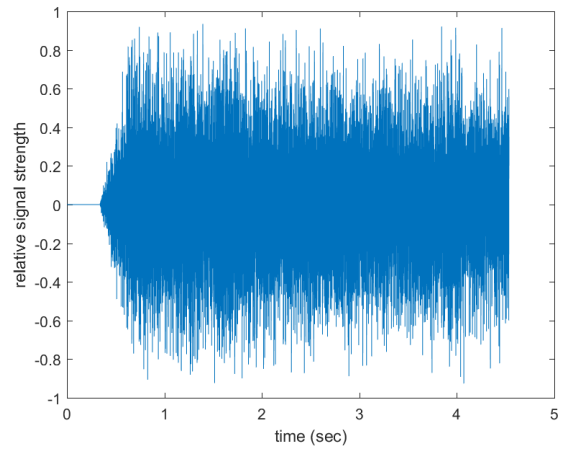

(a)

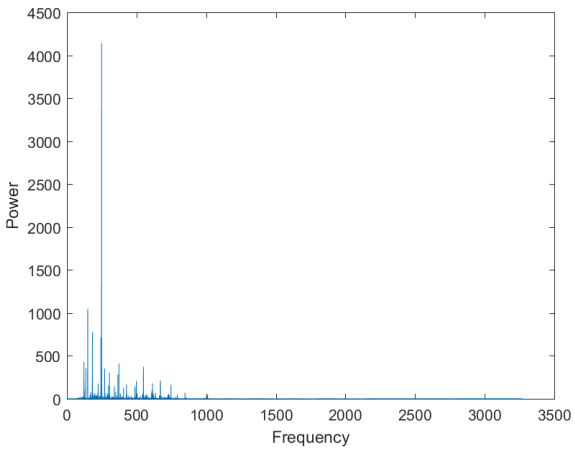

(b)

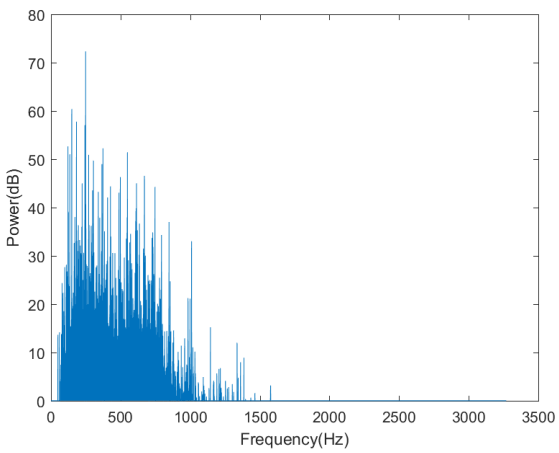

(c)

Fig. 3. An example of an acoustic signal with a length of 4.5 seconds. (a) signal in the time domain, (b) Power spectrum components, (c) Power spectrum in decibels (dB)

The sum of the errors caused by the measurement and definition of the structure is indicated by e_t. In the least squares method, the goal is to estimate the parameters so that the sum of squared error ($\sum {e_t}^2$) is minimized [24].

TABLE 4
DIMENSION REDUCTION ALGORITHM

Input: Data Matrix $X_{M\times N}$

1- *Compute the covariance of the matrix* $X_{M\times N}$ *:* $covarianceMatrix = cov(X)$
2- *Extract the eigenvectors of the covariance matrix:* $[V, D] = eig(covariance\ Matrix)$
3- *Show the new data in principal component space:* $Y = X * V$

Output: Data Matrix $Y_{M\times p}$ *in Principal component space where* $p < N$

In this method, a linear structure for the relationship between input and output is in the following form:

$$y_t = u_t^T\theta + e_t \tag{10}$$

where y_t is the output at t, θ is vector parameters, and u_t is a vector containing system information. In this method, $S = \sum {e_t}^2$ must be minimized to calculate θ. Therefore, the linear regression equation for all sampling times is as follows:

$$\begin{cases} y_1 = u_1^T\theta + e_1 \\ y_2 = u_2^T\theta + e_2 \\ \vdots \\ y_N = u_N^T\theta + e_N \end{cases} \tag{11}$$

The equation (11) will be in the following form:

$$y = U.\theta + e;\ \begin{cases} y_{N\times 1} = [y_1\ y_2\ \dots\ y_N]^T \\ U_{N\times p} = [u_1\ u_2\ \dots\ u_N]^T \\ e_{N\times 1} = [e_1\ e_2\ \dots\ e_N]^T \\ \theta_{p\times 1} = [\theta_1\ \theta_2\ \dots\ \theta_p]^T \end{cases} \tag{12}$$

Therefore, $\hat{\theta}$ (estimated parameters) is calculated as follows:

$$S = \sum_{t=1}^{N} {e_t}^2 = [y - U.\theta]^T[y - U.\theta] = y^Ty - \theta^TU^Ty - y^TU\theta + \theta^TU^TU\theta$$
$$\Downarrow$$
$$\frac{\partial S}{\partial \theta} = -2U^Ty + 2U^TU\theta \tag{13}$$
$$\Downarrow$$
$$\hat{\theta} = (U^TU)^{-1}.U^Ty.$$

Inverting (U^TU), when $\det(U^TU)$ is close to zero, can cause errors in $\hat{\theta}$ calculation [25]. In this case, it is called an ill-posed matrix. Therefore, alternative methods should be used to calculate the inverse of (U^TU). In this article, the singular value decomposition (SVD) method is used to solve this problem. The summary of the SVD method is shown in Table 5. The singular value decomposition of U is as follows [15]:

$$U_{N\times p} = P_{N\times N}R_{N\times p}Q_{p\times p} \tag{14}$$

where P and Q are orthonormal matrices with the following characteristics:

$$P^TP = PP^T = I_{N\times N}$$
$$Q^TQ = QQ^T = I_{p\times p} \tag{15}$$

And matrix R is in the following form:

$$R = \begin{bmatrix} \sigma_{p\times p} \\ 0_{(N-p)\times p} \end{bmatrix}_{N\times p} = \begin{bmatrix} \sigma_1 & 0 & \dots & 0 \\ 0 & \sigma_2 & \dots & 0 \\ \vdots & \vdots & \ddots & \vdots \\ 0 & 0 & \dots & \sigma_p \\ & & \mathbf{0} & \end{bmatrix}_{N\times p} . \quad (16)$$

Equation 12 can be written in the following form:

$$P^T.(y = U.\theta + e) \Rightarrow P^T y = P^T U\theta + P^T e$$

$$U = PRQ \Rightarrow P^T y = P^T PRQ\theta + P^T e \quad (17)$$

Where $PP^T = I$ and assuming $y^* = P^T y$, $e^* = P^T e$, $\theta^* = Q\theta$, (17) can be written in the following form:

$$y^* = R\theta^* + e^*. \quad (18)$$

To calculate θ^*, equation (18) is expanded as follows:

$$\begin{bmatrix} y_1^* \begin{Bmatrix} y_1^* \\ y_2^* \\ \vdots \\ y_p^* \end{Bmatrix} \\ y_2^* \begin{Bmatrix} y_{p+1}^* \\ \vdots \\ y_N^{*N} \end{Bmatrix} \end{bmatrix} = \begin{bmatrix} \sigma_1 & 0 & \dots & 0 \\ 0 & \sigma_2 & \dots & 0 \\ \vdots & \vdots & \ddots & \vdots \\ 0 & 0 & \dots & \sigma_p \\ 0 & 0 & 0 & 0 \\ 0 & 0 & 0 & 0 \end{bmatrix} \begin{bmatrix} \theta_1^* \\ \theta_2^* \\ \vdots \\ \theta_p^* \end{bmatrix} + \begin{bmatrix} \begin{Bmatrix} e_1^* \\ e_2^* \\ \vdots \\ e_p^* \end{Bmatrix} e_1^* \\ \begin{Bmatrix} e_{p+1}^* \\ \vdots \\ e_N^* \end{Bmatrix} e_2^* \end{bmatrix}. \quad (19)$$

$$\Downarrow$$

$$\begin{cases} y_1^* = \sigma_{p\times p}\theta^* + e_1^* \\ y_2^* = e_2^* \end{cases}$$

Therefore, $\theta^* = (\sigma^{-1} y_1^*)$ and using $\hat{\theta} = (Q^T\theta^*)$, $\hat{\theta}$ is calculated. Consequently, for modeling using the least squares method, the information matrix U is first calculated at different sampling times. The model parameters are estimated using the SVD method.

III. Practical Tests and Results

In this part, the experiments for modeling purposes were designed based on the factorial method and relative response time [26]. According to the previous description, for modeling the relationship between ground particle size and acoustic signal, before and after ball charging, the output (ground particles) of the ball mill is sampled at different times, and the acoustic signal is also recorded. Each sample is dried in the laboratory, and the sieve analysis is performed. In this section, the ASTM (American Standard Test Sieve Series) series and the Wet Sieve Analysis method are used for PSD (Particle Size Distribution) analysis. D_{80} is a characteristic diameter extracted from PSD and will be used in this section. Therefore, in the laboratory, 200 grams of the sample was separated, and the rest was stored as an archive. The representative sample was sieved on several different sieves. The material left on the first sieve should not be less than 10% of the total sample. If there is no load on it, a smaller sieve should be selected.

TABLE 5
SVD METHOD

Input: Matrix U

1- *Calculate the SVD of U: $U = PRQ$.*
2- *Calculate $y^* = P^T y$ and get y_1^*.*
3- *Calculate $\theta^* = (\sigma^{-1} y_1^*)$.*
4- *Calculate $\hat{\theta} = (Q^T\theta^*)$.*

Output: $\hat{\theta}$

Then, the amount of the remaining materials on each sieve is weighed, and the numbers are placed in a table along with the sieve number. Finally, graphs are drawn based on the data of the 80% of the material passed through the sieve, and the results are interpreted. Fig. 4 shows the sampling and analysis steps, respectively, in the plant and the laboratory. In the next part, the optimal load of the ball mill will be selected through sieve analysis for a better release of minerals.

A. Sieve Analysis Results

For a better release of each mineral, it is necessary to grind the input load to a specific size. In the studied plant, this value is in the range of 110 to 120 microns. Therefore, the feed rate is optimal when the ball mill can grind it to the intended size range. This range is specific to this factory, due to the specifications of its available facilities, and can be different in other places. The ground particle size results for different feed rates, before and after ball charging, are shown in Table 6, Table 7, and Fig. 5. Feed rate changes have a direct effect on retention time. If the feed rate increases, the retention time will decrease. With the rise in the feed rate, the retention time will be reduced, and less grinding will be done on the materials. Consequently, the output particle size will be coarser. According to the tests done in this part, the retention time was estimated to be between 8 and 15 minutes. Therefore, the sampling time of 42 minutes was selected based on the Nyquist theorem and retention time [27]. According to the Nyquist theorem, the signal sampling frequency should be chosen so that the vital signal data cannot be disturbed. During this time, it is expected that the output will reach stability in all different input tonnages. Also, all the data resulting from the grinding steps and fluctuations (used in modeling) can be seen in the output samples. According to Fig. 5, before the ball charging, a peak is observed in the 20t/h graph. It shows that this cargo is relatively large for the ball mill available in the factory, and the power of the ball mill to grind the load is small.

As a result, the output of the ball mill in the mentioned tonnage has a coarser particle size than other tonnages; therefore, the value of 20t/h is the critical value. Also, it can be concluded that the ball mill shows a better grinding performance at low tonnages.

Fig. 4. Sampling and sieve analysis steps

Therefore, the corresponding ground particle size curves are always downward over time. This process continues until the particles soften, and gradually, the curves become horizontal. Unlike the other charts, the 10t/h chart has less fluctuation and smaller particle size. As a result, it is better for the release of minerals. After charging new balls, the changes in all input tonnages decreased. In the previous chart, the feed rate of 20t/h is considered a critical feed rate due to the coarseness of the output particles even after the stability time. Compared to the other charts, the 10t/h chart has less fluctuation and a smaller particle size. Therefore, according to the analysis and requested size range, the optimal feed rate for the ball mill is 10t/h.

B. Spectral Analysis Results

In this part, to investigate the sound signal behavior at different feed rates, the signal power spectrum was calculated using (20) and (21). In the mentioned equations, $Y(k)$ is the FFT of $Y(t)$ (acoustic signal), and N is the signal dimension. Also, equation (21) calculates the power in decibels (dB).

$$Power = \frac{1}{N}\sum_{k=1}^{N}|Y(k)|^2 \tag{20}$$

$$Power(dB) = 20log_{10}(\frac{1}{N}\sum_{k=1}^{N}|Y(k)|^2) \tag{21}$$

Fig. 6 shows the power spectrum for three different feed rates, including 5t/h, 10t/h, and 20t/h. In this figure, the top row shows the components of the power spectrum, and the bottom row is the power spectrum in decibels (dB). According to Fig. 6, in the feed rate of 5t/h, the power spectrum is in a higher frequency range than the other two feed rates. In this load, the amplitude of power components is also more extensive than the other two loads. The reason is that when the feed rate is low, balls hit the mill body more frequently, and consequently, the intensity and frequency of the produced sound will be higher.

TABLE 6
PSD ANALYSIS (D_{80} RESPONSE BEFORE BALL CHARGING (MICRON))

	Feed Rate			
Time (min)	5t/h	10t/h	15t/h	20t/h
3.5	769	685	705	580
7	710	660	689	490
10.5	673	539	576	510
14	500	450	476	570
17.5	439	386	410	620
21	370	330	378	640
24.5	310	285	303	665
28	280	240	279	650
31.5	235	186	234	680
35	215	165	195	615
38.5	198	143	168	570
42	160	120	135	580

TABLE 7
PSD ANALYSIS (D_{80} RESPONSE AFTER BALL CHARGING (MICRON))

	Feed Rate			
Time (min)	5t/h	10t/h	15t/h	20t/h
3.5	340	321	334	510
7	290	276	289	473
10.5	257	245	259	435
14	276	227	246	450
17.5	220	214	229	439
21	210	196	210	439
24.5	203	184	201	432
28	198	181	193	424
31.5	192	168	175	412
35	181	152	167	406
38.5	162	131	143	393
42	143	112	127	387

In the feed rate of 20t/h, due to the high load of the machine, the sound resulting from the collision of the balls with the load is muffled. Therefore, in this case, the frequency of the power spectrum is shallow, and the amplitude is less than in the previous point. In the feed rate of 10t/h, the signal's frequency is in the middle band, and the amplitude of the power spectrum is also lower. This means that the mill is working normally, and the frequency and intensity of the sound are also suitable. Therefore, the summary of this part of the studied ball mill is as follows:

- The frequency range of the power spectrum for all cases is from 100 to 1300 Hz.
- If the feed rate is low, the sound power spectrum will be at higher frequencies, which is in the range of 700 to 1300 Hz.

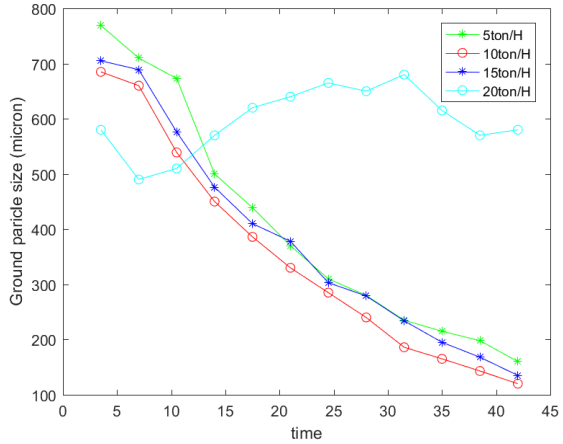

(a)

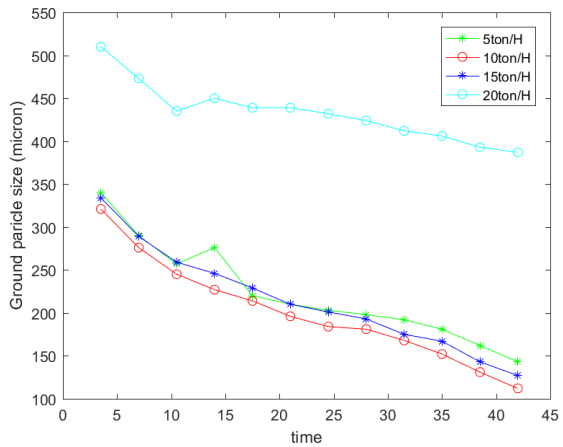

(b)

Fig. 5. PSD Analysis (Ground particle size (D_{80}) graph).
(a) before ball charging, (b) after ball charging

- If the feed rate is high (critical), the sound power spectrum will be at low frequencies, which is in the range of 100 to 300 Hz.
- If the feed rate is standard, the sound power spectrum will be in the middle frequencies and the range of 300 to 700 Hz.

Therefore, according to the results and the frequency range obtained for the sound, the feed rate of the ball mill can be divided into three states: standard feed rate, low feed rate, and critical feed rate.

C. Modeling Based on Least Squares

As mentioned in the previous sections, four features (including the maximum and minimum sound intensity in the time domain, and the amplitude and frequency of the maximum power spectrum components) are extracted as candidates from the acoustic signal in different time intervals.

According to Table 4, two features (i.e., the maximum and minimum sound intensity in the time domain) were ignored due to their low change interval. The reason is that to reduce the dimensions of the features (Table 4), the PCA-based method has been used. In this method, characteristics with more changes are considered more important in modeling. On the other hand, according to the obtained results, the range of changes in maximum and minimum sound intensity is tiny. The remaining two features used for modeling included the amplitude (A_m) and frequency (f_m) of the most significant component of the power spectrum.

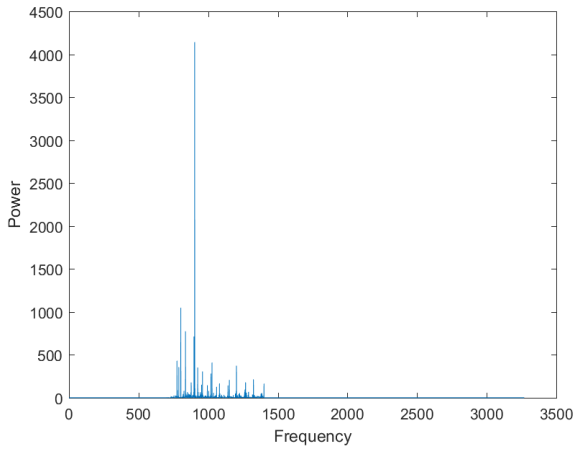

(a)

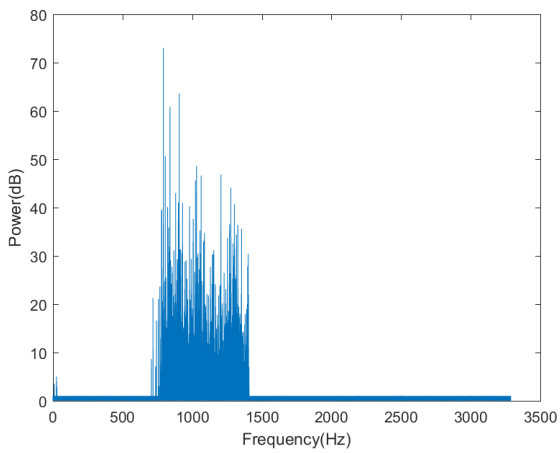

(b)

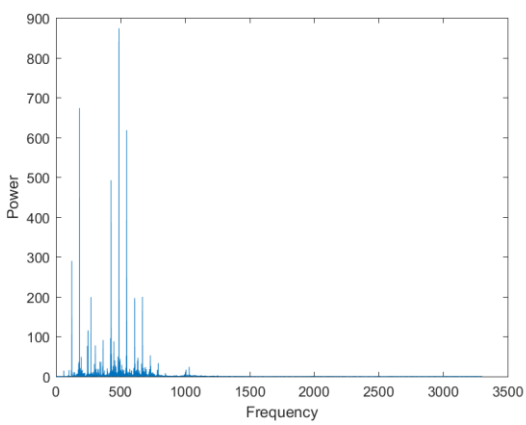

(c)

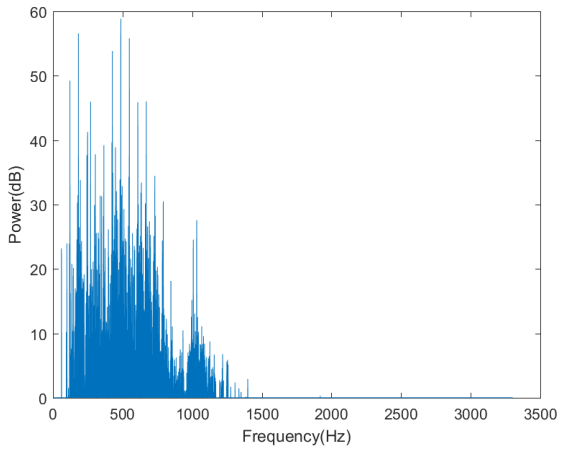

(d)

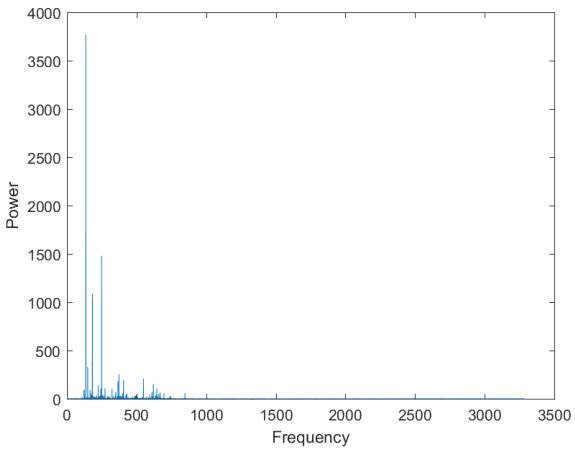

(e)

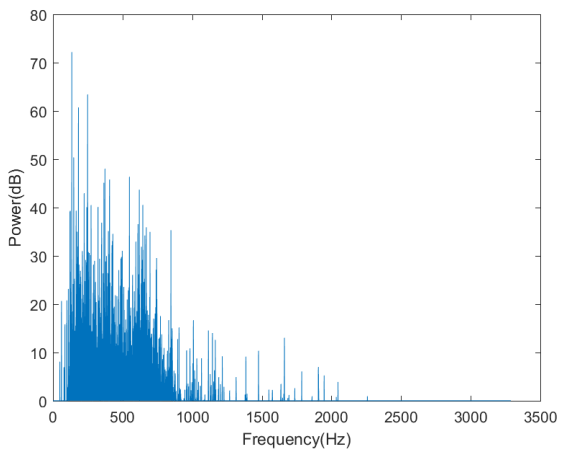

(f)

Fig. 6. Acoustic power spectrum at different feed rates (a),(b) low feed rate (5t/h) , (c),(d) standard feed rate (10t/h), (e),(f) high feed rate (20t/h)

In this article, the goal is to find a model that shows the relationship between the ground particle size and the audio signal. To achieve this goal, A_m and f_m are extracted from sound in all sampling time intervals. Then, the ratio f_m/A_m is innovatively used as a feature extracted from the sound. Sound is the result of vibration. This ratio can physically express the amount of vibration resulting from the collision of the balls with the ore. Using this feature, critical and standard conditions of the mill can be identified. According to the amount of vibration created in the ore, the normal and vital conditions of the mill will be determined, and a specific sound frequency range will be produced. In section 3.1, the ground particle size for all samples has been extracted using sieve analysis. Therefore, according to section 2.4, a mathematical model can be obtained by putting the ground particle size on the Y-axis and the feature value on the X-axis. In this study, the least squares method based on polynomials has been used.

The polynomial degree selection is one of the primary challenges in modeling. It should be noted that the purpose of modeling is not to predict the output for the given data; instead, it is to predict the outcome of the unseen data. A model that makes reasonable predictions on new unseen data has generalization ability. A simple and effective method to determine if a model can be generalized is to divide the original data into a training set and a test set. Therefore, 80% of the data is used for training and 20% for model testing. After polynomial modeling with different degrees, the value of RMSE is calculated using (22). In this equation, Y_i is the actual value of the data, and $\hat{Y}_i$ is estimated by the model.

$$RMSE = \frac{1}{N}\sum_{i=1}^{N}(Y_i - \hat{Y}_i)^2 \tag{22}$$

Then, the RMSE diagram is drawn for the training and test data in different degrees in polynomial equations. Finally, the degree with the lowest RMSE value in the test data is selected as the most preferable one. In Fig. 7, the model validation is done for the data before and after the ball charging. According to this figure, degrees 2, and 3 are reasonable choices. Given the trade-off between simplicity and accuracy, degree 2 is chosen for modeling.

The modeling results for the feed rate of 10t/h before and after ball charging are shown in Fig. 8 and Table 8. Using this model, the ground particle size is estimated based on the feature value extracted from the sound. Therefore, the control plan (Fig. 2) of the ball mill will be as follows:

- First, the optimal feed rate (i.e., 10t/h) is set, based on the previous results.
- Then, the mill sound signal is recorded every 3.5 minutes, after the retention time (15min).
- After the noise removal process, the features and the sound power spectrum are extracted.

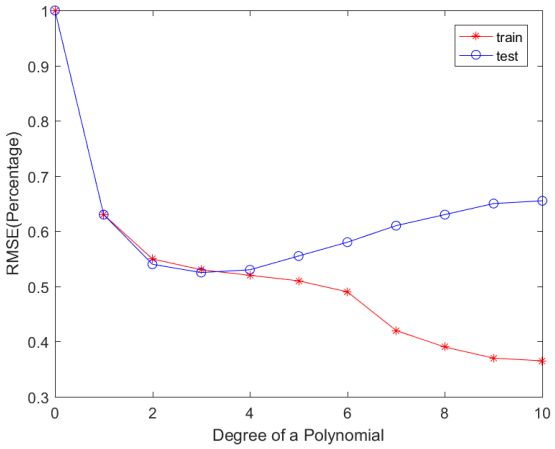

(a)

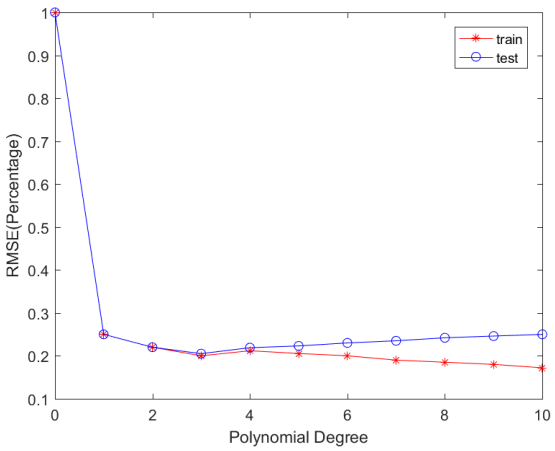

(b)

Fig. 7. Model validation chart
(a) before ball charging, (b) after ball charging

- Using the extracted features, the ground particle size is calculated.
- If the calculated ground particle size is 10% different from the desired one and the sound power spectrum is not in the middle-frequency range, the feed rate value should be changed.

D. Built-in Control Device

Fig. 9 shows installing the microphone and adjusting the feed rate to the ball mill in the Lakan lead-zinc processing plant. The microphones are installed in a place closest to the bottom of the mill. In this article, a BY-M1 BOYA condenser microphone was used for recording the sound.

Due to the high quality and sensitivity of the condenser microphones, more details of the signal are recorded, and the sampled signal can be used to diagnose the working conditions of the ball mill.

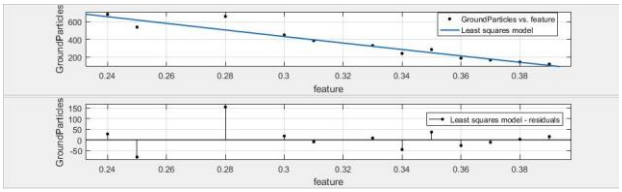

(a)

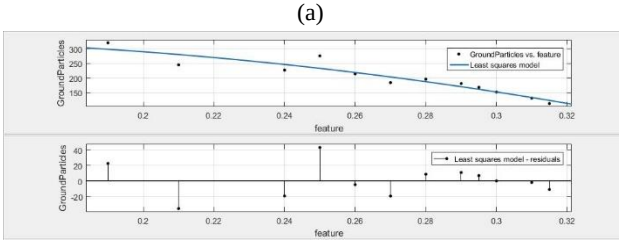

(b)

Fig. 8. Modeling based on least squares before and after ball charging in feed rate 10t/h
(a) before ball setting, (b) after ball charging

TABLE 8
The identified model in Fig. 8

Before Ball Charging: $f(x) = p_1x^2 + p_2x + p_3, \quad p_1 = 1.859,\ p_2 = -182.1,\ p_3 = 339.6$ RMSE= 54.97
After Ball Charging: $f(x) = p_1x^2 + p_2x + p_3, \quad p_1 = -4817,\ p_2 = 1029,\ p_3 = 276.9$ RMSE= 22.99

The control plan proposed in this article (Fig. 2) can be implemented in two ways. One is to use a computer and connect a microphone to it so that the received signal can be analyzed using the proposed method in MATLAB software. Using this method, the ground particle size is calculated, and the feed rate is changed if needed. In the other way, a unique device is made using an Arduino microcontroller (Fig. 10 shows different parts of the manufactured device). In the mentioned circuit, the received audio signal is first amplified using an analog amplifier. In the next step, the signal is transferred to the microprocessor. Then, the signal is denoised, and features are extracted. After that, the ground particle size is estimated using the extracted models in Fig. 8, and the sound power spectrum is also calculated. If the ground particle size and sound power spectrum condition are not ideal (according to 3.2), the buzzer starts making sounds, and the control switch is turned on to change the feed rate. In this article, both methods were practically implemented. In the first method, the cost of implementation and construction is high, but the data processing power is much higher than in the second method.

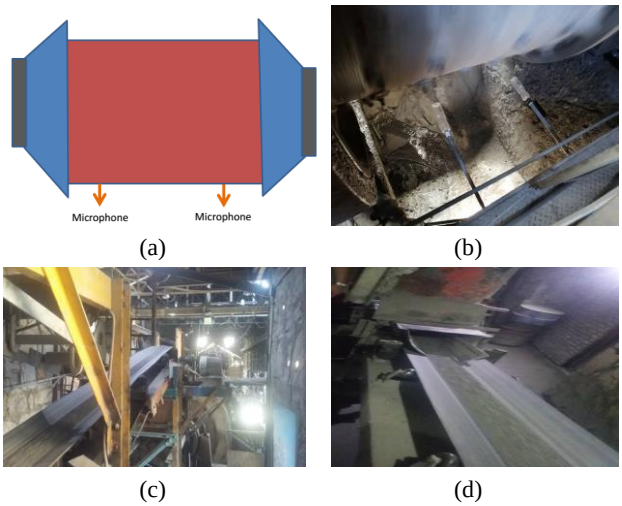

(a) (b)

(c) (d)

Fig. 9. Installing the microphones near the mill floor and adjusting the input feed rate. (a) Location of microphones, (b) Microphone installation in the plant, and (c), (d) Setting the feed rate

However, in the second method, the manufactured device is portable and, hence, cost-effective due to its small dimensions. The fabricated device can reduce the energy consumption of the ball mill. Also, by adjusting the optimal feed rate, the average size of ground products can be decreased and set in the appropriate range. In the proposed control system, since the ball mill load is standard, ball mill energy consumption will be optimal. Optimal load control will also increase the ball charging time. Therefore, a smaller number of balls will be used. Consequently, the system designed in this article will increase the efficiency of the ball mill in practice. As explained in the introduction section, the studied ball mill liner is made of plastic. Metal liners produce a lot of noise, and distort the sound resulting from the collision of the balls with the particles. But plastic liners do not make noise due to their elasticity. Therefore, the received sound will result from the impact of the material with the balls. Hence, one of the limitations of the proposed method is that the liners must be plastic to minimize the error. Because of the fact that nowadays, plastic liners are primarily used in ball mills, the presented method will not have severe limitations. One of the most essential points in the designed system is repeatability. To achieve it, the identified model should be updated as the system parameters change. For this purpose, in the new device version, the modeling process is done in different time frames. Using this method, the model is continuously updated. To do so, the output ground particles are analyzed using a CAMSIZERX2 device. Particle size distribution data (i.e., D_{80}) is sent to the device online. Then, the modeling process is done based on the least square error method, and the model will be updated.

IV. Conclusion

In this study, an innovative combined method was implemented to control the ground particle size and load of the ball mill. In this method, the relevant modeling was first done using both the acoustic signal and the ground particle size diagram.

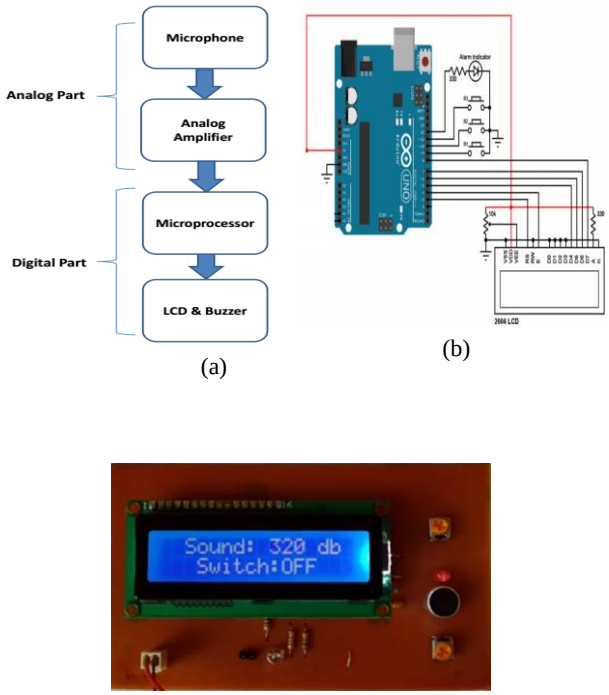

(a) (b)

(c)

Fig. 10. Prototype of the ball mill control device. (a) schematic of the device, (b) a digital circuit, (c) a prototype of the manufactured device

To do so, the output (ground particles of the ball mill) was first sampled, and the acoustic signal acquisition process was also performed. After the sieve analysis, the ground particle size diagram was drawn. In the next step, using the new method of quantum adaptive basis, the acoustic signal outliers were removed. Then, the Fourier transform of the signal and the power spectrum were calculated. Four features, namely the maximum and minimum values of the sound in the time domain, and the maximum of the power spectrum component (amplitude and frequency), were extracted from the acoustic signal. In the next step, a PCA-based method was applied to reduce the dimension of the features. Finally, the regression model between sound signal and ground particle size was obtained using the least squares method. This model is also used to control the ball mill. The resulting model can detect the ground particle size and load status (standard, low, high) by recording the sound of the ball mill, when in operation. In this article, all the steps of the proposed method were practically tested on the ball mill of the Lakan lead-zinc processing plant. Also, a device that controls the ground particle size and ball mill load was built. According to the results, the optimal feed rate for the ball mill is 10t/h. In this case, the size of the ground particles is suitable (110-120 microns), and the sound power spectrum is 300-700 Hz. It should be noted that the optimal

feed rate obtained in this article is only specific to the studied ball mill. That is, the optimal feed rate in other factories might be different, and it must be calculated using the proposed scheme. According to the analysis and results of the study, the proposed control plan will reduce the energy consumption of the ball mill and increase the ball charging time. Therefore, the proposed method will increase efficiency in this factory. The authors of this article aim to measure the amount of energy and the number of balls saved in this process for their future research**.** Also, the modeling of more complex ball mill systems will be investigated in the following study.

References

[1] S. Singh, S. K. Singh, P. K. Harijan, S. K. Yadav, and A. Kumar, "Investigation on the effect of Fe impurity pickups during ball milling and Ni dispersion on the microwave absorption performance of ball milled Fe impurities-Ni/SiC composites," Journal of Materials Science: Materials in Electronics, Jul. 2022.

[2] A. Hajati, S. Shafaei, & M. Noaparast, "A novel approach to optimize grinding circuits-modelling strategy to monitor ball mill particle size distribution data at Lakan plant, " IJST, Transactions of Mechanical Engineering, vol. 35, pp.85-100, 2011.

[3] A. M. Tsirlin and A. I. Balunov, "Optimal Control of Technological Processes," Processes, vol. 11, no. 6, pp. 1835–1835, Jun. 2023.

[4] Y. Li, "Modelling tumbling ball milling based on DEM simulation and machine learning," (Doctoral dissertation, UNSW Sydney), 2023.

[5] K. S. Cho, S. Kim, and Young Hun Lee, "Correlation between Acoustic Intensity and Ground Particle Size in Alumina Ball Mill Process," Journal of The Korean Ceramic Society, vol. 55, no. 3, pp. 275–284, May 2018.

[6] J. Lv, Z. Wang, and S. Ma, "Calculation method and its application for energy consumption of ball mills in ceramic industry based on power feature deployment," Advances in Applied Ceramics, vol. 119, no. 4, pp. 183–194, Feb. 2020.

[7] Halit Sübütay and İlyas Şavklıyıldız, "Effect of High-Energy Ball Milling in Ternary Material System of (Mg-Sn-Na)," Crystals, vol. 13, no. 8, pp. 1230–1230, Aug. 2023.

[8] Shashi Prakash Dwivedi et al., "Effect of ball-milling process parameters on mechanical properties of Al/Al2O3/collagen powder composite using statistical approach," vol. 15, pp. 2918–2932, Nov. 2021.

[9] J. Tang, J. Qiao, Z. Liu, X. Zhou, G. Yu, and J. Zhao, "Mechanism characteristic analysis and soft measuring method review for ball mill load based on mechanical vibration and acoustic signals in the grinding process," vol. 128, pp. 294–311, Nov. 2018.

[10] J. Shi, G. Si, and Y. Zhang,"Application of Fractional Fourier Transform for Prediction of Ball Mill Loads Using Acoustic Signals," IEEE Access, Jan. 2019.

[11] X. Wang, K. Sun, H. Zhang, X. Wan, and C. Yang, "Mill Load Identification Method for Ball milling Process Based on Grinding Signal," IFAC-PapersOnLine, vol. 54, no. 21, pp. 7–12, Jan. 2021.

[12] Y. Li, J. Bao, T. Chen, A. Yu, and R. Yang, "Prediction of ball milling performance by a convolutional neural network model and transfer learning," Powder Technology, vol. 403, p. 117409, May 2022.

[13] S. Kalantari, M. Ramezani, A. Madadi, and V. V. Estrela, "Reduction AWGN from Digital Images Using a New Local Optimal Low-Rank Approximation Method," Smart innovation, systems and technologies, Dec. 2020.

[14] C. Tian, M. Zheng, W. Zuo, B. Zhang, Y. Zhang, and D. Zhang, "Multi-stage image denoising with the wavelet transform," arXiv (Cornell University), Sep. 2022.

[15] S. Kalantari, M. Ramezani, and A. Madadi, "Introducing a New Hybrid Adaptive Local Optimal Low Rank Approximation Method for Denoising Images," International Journal of Industrial Electronics Control and Optimization, vol. 3, no. 2, pp. 173–185, May 2020.

[16] S. Kalantari, A. Madadi, & M. Ramezani, "Reconstruction of Geological Images Based on an Adaptive Spatial Domain Filter: An Example to Introduce Quantum Computation to Geosciences," International Journal of Mining and Geo-Engineering, vol. 57, no. 2, pp. 183-194, 2023.

[17] Muhammad Sahimi and Pejman Tahmasebi, "The Potential of Quantum Computing for Geoscience," Transport in Porous Media, vol. 145, no. 2, pp. 367–387, Sep. 2022.

[18] S. Dutta, A. Basarab, Bertrand Georgeot, and D. Kouamé, "Quantum Mechanics-Based Signal and Image Representation: Application to Denoising," IEEE open journal of signal processing, vol. 2, pp. 190–206, Jan. 2021.

[19] P. W. Anderson, "Absence of Diffusion in Certain Random Lattices," Physical Review, vol. 109, no. 5, pp. 1492–1505, Mar. 1958.

[20] S. Kalantari and M. J. Abdollahifard, "Optimization-based multiple-point geostatistics: A sparse way," Computers & Geosciences, vol. 95, pp. 85–98, Oct. 2016.

[21] H. Liu, J. Zhang, and R. Xiong, "CAS: Correlation Adaptive Sparse Modeling for Image Denoising," IEEE transactions on computational imaging, vol. 7, pp. 638–647, Jan. 2021.

[22] E. Rajaby and S. M. Sayedi, "A structured review of sparse fast Fourier transform algorithms," Digital Signal Processing, vol. 123, p. 103403, Apr. 2022.

[23] B. Hasan, B. M. S., & A. Abdulazeez, "A review of principal component analysis algorithm for dimensionality reduction," Journal of Soft Computing and Data Mining, vol. 2, pp. 20-30, 2021.
[24] Z. Raisi, & J. Zelek, "Investigation of Deep Learning Optimization Algorithms in Scene Text Detection," International Journal of Industrial Electronics Control and Optimization, 2023.
[25] J. P. Norton, "An introduction to identification," Courier Corporation, 2009.
[26] C. J. Miller, S. N. Smith, and M. Pugatch, "Experimental and quasi-experimental designs in implementation research," Psychiatry Research, vol. 283, no. 112452, Jun. 2019.
[27] J. Hamill, G. E. Caldwell, and T. R. Derrick, "Reconstructing Digital Signals Using Shannon's Sampling Theorem," Journal of Applied Biomechanics, vol. 13, no. 2, pp. 226–238, May 1997.

Sadegh Kalantari was born in Tafresh, Iran. He received his B.S. and M.S. degrees in electrical engineering from Tafresh University. He is currently a Ph.D. candidate in control engineering at Tafresh University. His current research interests include system identification, optimization, signal processing, quantum control, quantum computing, geostatistics, and machine learning.

Ali Madadi received a Ph.D. degree in control engineering from the Amirkabir University of Technology. He is an associate professor in the Department of Control Engineering, at Tafresh University. His current research interests include optimal control, robust control, adaptive control, nonlinear control, optimization, and system identification.

Mehdi Ramezani received a Ph.D. in applied mathematics and optimal control from the Amirkabir University of Technology. He is an assistant professor in the Department of Mathematics at Tafresh University. His research interests include optimal control, system identification, optimization, control, soft computing, and machine learning.

Abdolmotaleb Hajati received a Ph.D. degree in mining engineering from Tehran University. He is an assistant professor in the Department of Mining Engineering at Arak University of Technology. His current research interests include nanoflotation and mineral processing.